

KASR EL - AINI

MEDICAL JOURNAL

Chairman of the Editorial Board:

Prof. Saleh Bediar

General Manager:

Prof. Nadia Hassan Badrawi

Editor in Chief:

Prof. Zakaria Abdel-Hamid



SONOGRAPHIC TISSUE SIGNATURE OF BRIGHT LIVER

Laila A., MD*, Ashraf Omar Abdelaziz, MD*... Ahmed M. Badawi**, Ph.D.,
Ahmed M. Salama, MSc* and A. M. Youssef**

*Tropical Medicine Dept., Faculty of Medicine, Cairo University

** Biomedical Engineering, Cairo Univ., Faculty of Eng. Cairo University

ABSTRACT:

Background: Computerized ultrasonographic tissue characterization has become an objective means for diagnosis of liver diseases. It is difficult to differentiate diffuse liver diseases by visual inspection from the ultrasound images. Computerized ultrasonographic tissue characterization has emerged as one of the most accurate methods in classification of different liver pathologies.

Aim of the work: Is to establish a specific quantitative criteria for computerized discrimination of different diffuse liver diseases detected as bright liver by ultrasound.

Materials and Methods: Using 10 tissue characterization parameters namely; mean gray level, 9th percentile, contrast, entropy, attenuation, correlation, angular second moment, average specular intensity, average diffuse intensity and speckle separation distance was able to differentiate between different hepatic pathologies among 45 patients with sonographically detected bright liver and of known histopathological data as well as 12 control subjects. A neural network model is proposed to classify different diseases from detecting these quantitative parameters from the ultrasound images. **Results:** We reported a results of classification of bright livers of 91.11% sensitivity, specificity 100%, and accuracy 92.72% ..

Conclusion: We can conclude that, Computer-assisted sonographic tissue characterization using the neural network classifier is a sensitive and specific technique for separating diffuse liver disease with ultrasonically detected bright liver from control cases. This will be of great benefit to avoid invasive methods in unfit hepatic patients.

Key words: Ultrasonography, Tissue characterization, Bright liver, chronic hepatitis, Fatty liver, Cirrhosis, Neural network classifier and diffuse liver diseases.

INTRODUCTION:

Chronic liver diseases constitute a major health problem in Egypt. Nowadays viral hepatitis competes with schistosomiasis as a leading cause of chronic liver diseases in Egypt and elsewhere in Middle East (*El-Roohy, 1985*). Ultrasonographically detected bright liver is a frequent finding commonly met with in patients with fatty liver, chronic hepatitis and cirrhosis (*Joseph et al., 1979*). Ultrasonography is particularly effective in identification of cystic lesions as they have no internal echoes and have sharp borders providing high contrast with the surrounding tissue, also it is effective in detection of focal hepatic lesions when they are more or less echogenic than the surrounding tissue (*Gara, 1991*). *Zwiebel (1995)* stated that ultrasonic imaging is not an accurate tool for the detection of diffuse liver disease. This may be due to subjective nature of sonographic interpretation which is error-prone for three reasons: first, disease processes may alter the echogenicity of the standards of comparison, the kidney and pancreas; second: interobserver variability is considerable and third: instrument setting variables may diminish or accentuate difference in echogenicity. These differences are partly responsible for the considerable interest shown in quantitative ultrasonic tissue characterization techniques. Tissue characterization is a term that refers to the quantitative estimation of tissue or image features leading to a more accurate distinction of normal from abnormal tissue. The results of tissue characterization may be quantitatively interpreted using numerical values or may be displayed as an image for qualitative interpretation by an observer. Tissue characterization aims to provide additional information about tissues not readily available by simple viewing of ultrasound B-scan. The information gained from tissue characterization is usually quantitative and is far less operator dependent than is the usual in B-scan image (*Gara, 1991*). The Visual criteria provides low diagnostic accuracy (around 70%) (*Youssef et al., 1993*). Therefore the physicians may have to use further invasive methods such as the pathology investigation of ultrasonically guided needle Biopsy. Although this technique is considered to be the golden test for diagnosis, it has the disadvantage of being invasive and risky, it may cause a great risk of cancer spread if it cuts through a localized cancer area (*Youssef et al., 1993, and Badawi et al., 1994*). The quantitative analysis of using ultrasound signals as an aid to the diagnosis of diffuse disease has been described by many researchers (*Badawi et al., 1996*). So the aim of this study is to establish a specific quantitative criteria for computerized discrimination of different diffuse liver diseases detected as bright liver by ultrasound.

MATERIALS AND METHODS:

Forty-five patients having bright liver on sonographic examination were selected from about 300 patients suffering from various liver diseases and 12 subjects served as control during the period from May 1997 to April 2000. All patients were from admission to Tropical Medicine Department and liver unit Kasr El Aini Hospital, Cairo University hospitals. They were 11 males and 34 females, their ages ranged from 27 to 65 years.

This work included two phases:

Phase I (Case study):

Including clinical, laboratory, conventional ultrasonography and pathological examination. Clinical examination includes general (Pulse, temperature, blood pressure, body measurements, cardiopulmonary, neurological, renal measurements) and local (liver, abdominal) examinations.

Laboratory investigations are :

1- Blood sugar 2- Complete blood picture 3- Liver function tests 4- Serological tests for hepatitis markers 5- Serum lipids 6-Serum auto-antibodies 7-Liver Biopsy for histopathological assessment

Phase II (Ultrasonographic tissue characterization) Including:

- I- Sonographic image analysis.
- II- Construction of the neural network.
- III- Testing the efficacy of the network.

I. Sonographic image analysis:

- a) Data acquisition system.
- b) System settings.
- c) Calculation of image parameters.

a) Data acquisition system:

The video output of an aTL Ultramark model 9 ultrasound machine was connected to a Nova-Microsonics workstation for image acquisition. The images were captured for fully inspired subject with controlled movement.

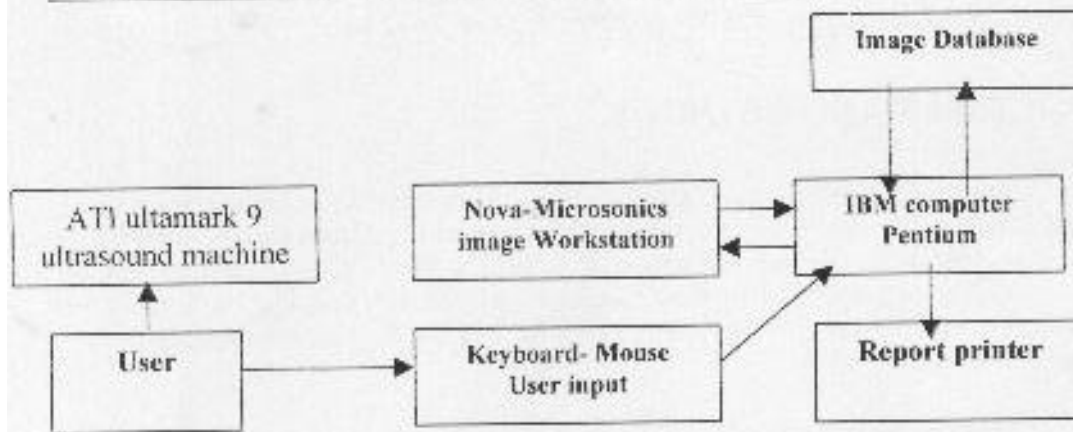


Figure 1: Block diagram for the developed system.

A software was developed on this system to allow the sonographer to define the region of interest (ROI) in the image for tissue characterization (WINDOWS operating system).

b) System setting:

To obtain reproducible results, the following parameters were standardized for all tissue characterization procedures from the B-mode image (Badawi, 1996).

1. **Ultrasound machine settings** e.g. Timed gain control (TGC), focus and zoom controls which can change the overall image gain and produce zooming effects and hence they can deviate the image statistics in unpredictable way. Moreover, the frequency of ultrasound waves used were the same for all subjects since the attenuation is frequency dependent.

2. **Region of interest: size and shape:** Region of interest is the part of the image where different analytical procedures are performed. Images were acquired in a transverse subcostal scan taken for the patient just preceding a needle liver biopsy. To obtain reliable statistics, the number of pixels in the region of interest must be at least a thousand pixels (1cm X 1cm = 30 X 30 pixels). A practical ROI size was 2cm X 2 cm, i.e. 60 X 60 pixels. Also, the square shape of the region should be maintained during all procedures.

3. **Region of interest location:** to avoid the distorting effects in ultrasonic wave patterns, the ROI should be selected each time along the center of the image. Also, it

should include pure texture i.e. away from major vessels.

4. **Fasting condition of the patient:** each study subject should be fasting for at least 8 hours before the scan to avoid the effect of changing liver glycogen and water storage on ultrasound attenuation.

c) Calculation of image parameters:

The simplest form of image data analysis is that of the pixel data histogram, which is a display of the occurrence frequency of gray levels in a region or along a line in the image.

The first order texture statistics: that is giving information about gray level frequencies but not about spatial location [e.g. mean gray level, 9th percentile]. This form of analysis has been implemented on several commercial ultrasonic imagers and usually allows calculation of the mean intensity value of the pixels along a given line of interest or from within a region of interest. Usually a histogram of the gray level distribution is displayed on the screen. Although this form of analysis has been available on many scanners, it has been little used since mean pixel gray level is strongly dependent on the gain settings used and no method for standardization or calibration of the intensity levels is usually available.

The second order parameters: the second order statistical features give not only occurrence frequencies of gray levels but also spatial interdependencies between the image elements (pixels). (e.g. contrast, angular second moment, entropy and correlation).

Acoustical parameters: e.g. Attenuation.

Speckle parameter namely; average specular intensity (Is), average diffuse intensity (Id) and speckle separation distance.

The parameters measured in our work included: mean gray level (MGL), 9th percentile (PER9), contrast (CON), entropy (ENT), correlation, angular second moment (ASM), attenuation (ATTEN), average specular intensity (IS), average diffuse intensity (ID) and speckle separation (sp sep) distance.

It is important to describe the gross discriminative effect of each of the most significant parameters used to build the on-line quantitative tissue characterization system (QTCS).

The MGL physical meaning is the brightness or echogenicity of texture, which most of the sonographers write in their ultrasound reports. It is well established that in fatty and cirrhotic livers the echogenicity is higher (*Behan et al., 1978*). The integration of the histogram will yield the distribution function from which we can extract the percentiles that express what is the gray level at which % of pixels has certain level i.e. for example from 0 to 255 gray level there are 90% of the gray level from 0 to 200, this is the 9th percentile.

Correlation is a measure of the linearity of the gray levels relationship in related pixels i.e. a measure of homogeneity.

Average diffuse intensity (ID), average specular intensity (IS) and specular separation "measured from ID and IS values" are textural parameters give information about the texture of the tissue. Attenuation is the amount of ultrasound wave decay by depth in given tissue.

Contrast (CON) is defined as a measure of how many large gray level differences are present in the region of interest. Frequently occurring large gray level differences increase the contrast value, whereas soft texture results in small contrast value (*Raeth et al., 1985*).

Angular second moment (ASM) and entropy (ENT) characterize the distribution of co-occurrence matrix entries in a gray level-independent way. ASM increases when the co-occurrence matrix values are clustering around a major gray level transition. This corresponds to a situation where only a small number of different gray level transitions exist. Entropy measures the homogeneity or uniformity of the tissue, and therefore it increases with increasing coarseness of the image texture (*Kudah et al., 1996*).

II. Construction of the Neural Network:

Neural networks are a special kind of flexible model. They consist of networks of elements, each element or node computes a weighted sum of its input and applies a function of some kind to generate an output, hence the analogy with neurons. Nodes are arranged in layers. The input layer receives input, which may be raw image data (as in our case), processed image data or information about the features of an interpreted image. The output layer provides the response of the system (the diagnosis in our case). Most neural nets used in object recognition system include a single "hidden" layer between the input and output.

To use the system for object recognition they must be first trained. Training consists of providing the system with examples of the possible input (different ultrasound images of various liver pathologies in our case) and allowing a control loop (e.g. feedback or feed-forward) to adjust the weights of the system's nodes to produce the required output. The system is considered a success if it is able to generalize what it has learnt and classify new examples correctly (*Badawi et al., 1996, Kadah et al., 1996*). (E.g. in the training phase the input layer receives the data $(x_1 \& x_2, \dots$ etc) that will be processed in the hidden layer (augmented by variable weights) to adjust the output toward the required output (required diagnosis).

In this work, feature extraction algorithms are proposed to extract the tissue characterization parameters from liver images. Then the resulting parameter were processed

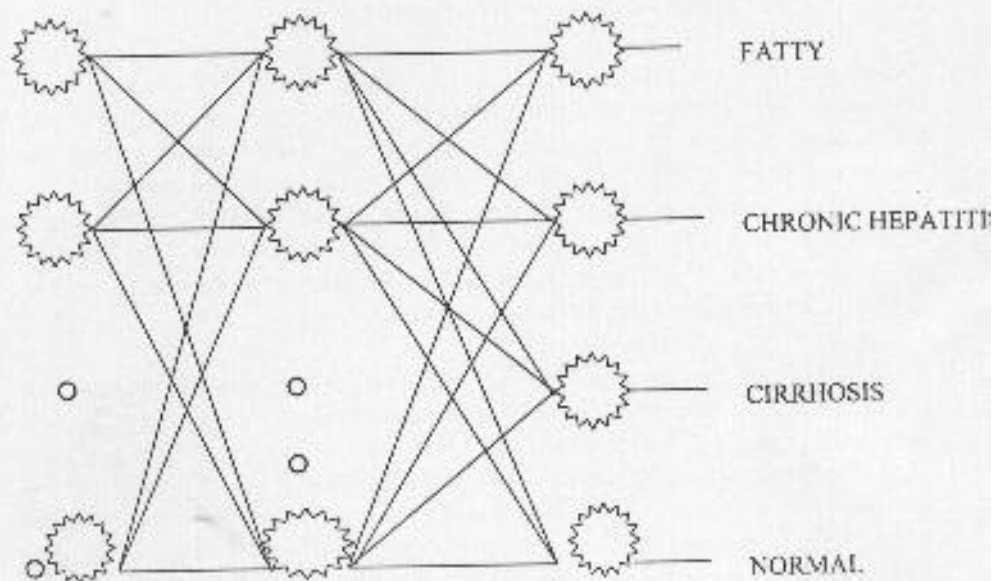


Figure 2: Neural network architecture for multilayer network.

as follows to construct the neural network:

- **Preprocessing:**

An important initial step in all algorithms is to cut the data set into two independent subsets namely, training and test sets.

The training set in our study included, 6 control subjects, 10 patients with fatty liver, 12 patients with chronic hepatitis and 4 cirrhotic patients while *the test set* included, 6 control subjects, 6 patients with fatty liver, 10 patients with chronic hepatitis and 3 cirrhotic patients.

This preliminary step effectively avoids introducing false-negative bias effects. Also, the effect of normalization of all parameter values within a fixed range around the zero (between ± 1) is studied as a possible convenient preprocessing step for proper weighing of parameters. This effectively help speeding up the training by moving the operating point to the linear portion of the neuron activation function,

which has the highest slope. Also, each of the possible pathologies is assigned a binary digit which can take only 2 values:

present/absent, which are mutually exclusive.

- **Training different multi-layer perceptron architectures:**

In these architectures, the network consists of a first (hidden) layer of variable number of perceptrons feeding a second (output) layer of size equal to the number of pathologies (4 groups in our study, namely; fatty change, chronic hepatitis, cirrhosis and control). Various hidden layer sizes were used and the output was produced by a binary or a maximum response decision criteria to decide one of the four pathologies. The algorithm used to train this class is the *Multi-Layer Back Propagation* training algorithm. We had 10000 iteration for learning. MSE was found to be 0.1. The learning factor was set to 0.3, the momentum term was used to accelerate training convergence and was set to 0.7. We applied a sigmoidal activation for all our neurons. We had a size of 20 neurons in the hidden layer as the optimal size that gave the least MSE results. We have built a special VC++ S/W for image processing and automatic diagnosis tasks with a simple to use GUI (Graphical User Interface).

III. Testing the efficacy of the network:

1-Test the network after training by classifying the samples from the test set and obtain the error rate for the network by calculating the percentage of the number of mis-classified samples to the total number of test samples.

2- Sensitivity, specificity and overall accuracy of the network were calculated.

Sensitivity is the proportion of subjects with the disease who have a positive test, indicating how good a test is at identifying the diseased.

It equals $[true\ positive / (true\ positive + false\ negative)] \%$.

Specificity is the proportion of subjects without the disease who have a negative test, indicates how good a test is at identifying the non-diseased.

It equals $[true\ negative / (true\ negative + false\ positive)] \%$.

Accuracy of a variable is the degree to which it actually represents what it is intended to represent.

It equals $[(true\ negative + true\ positive) / (true\ negative + false\ positive + true\ positive + false\ negative)] \%$.

RESULTS:

The results of this study were statistically analyzed and tabulated in tables 1 through table 18. Results of **phase I** (case study) are shown in table 1 through table 4. Results of **phase II** (tissue characterization) are shown in table 5 through table 15 and the results of testing the efficacy of the neural network **phase III** are shown in table 16 through table 18.

Table (1): Age distribution of 57 studied subjects:

	Patients No. (45)	Control No. (12)
Range (Ys.):	27-65 Ys.	16-65 Ys.
Mean \pm SD	39.044 \pm 7.73	39.1 \pm 13.9

Table (2): Sex distribution of 57 studied subjects:

Sex	No.	%	No	%
Females	34	75.6	9	75
Males	11	24.4	3	25

Table (3) Classification of the study group according to histopathological findings:

Findings	No	%
Fatty changes	16	35.6
Chronic hepatitis	22	48.9
• Chronic hepatitis.	6	13.3
• Chronic hepatitis & fatty change	16	35.56
Cirrhosis	7	15.
• Cirrhosis	3	6.66
• Cirrhosis & fatty change	4	8.89

Table (4) Clinical data in different pathological groups:

	Fatty change(16)		Chronic hep (22)		Cirrhosis (7)	
	No	%	No	%	No	%
Sex						
• Male	1	6.3	7	31.8	3	42.9
• Female	15	93.7	15	68.8	4	57.1
Overweight	13	81.3	14	63.6	5	71.4
Jaundice	0	0	10	45.5	5	71.4
Elevated ALT	1	6.3	8	36.4	3	42.9
Hep markers:						
*+ve HCV	3	18.8	15	68.2	3	42.9
*+veHBcAb	0	0	1	4.55	0	0
*+veHBsAg	0	0	3	13.64	2	28.6
*Anti-HCV&HBV+ve	0	0	3	13.64	2	28.6
Serum lipid:						
Elevated cholest.	10	62.5	3	13.6	3	42.6
Elevated TG	10	62.5	3	13.6	1	14.3
Elevated blood sugar	3	18.8	1	4.5	1	14.3

Table(4) Female to male ratio are high in all groups and highest among fatty group. According to body mass index (BMI), overweight patients (BMI 25-30 Kgm/m²) were noted mainly in fatty group (81.3%) while in cirrhotic patients (71.4%) overweight may associated with oedema and ascites. Jaundice is associated mainly with cirrhotic group (71.4%) and with chronic hepatitis group (45.5%). Elevated ALT is almost seen among patients with chronic hepatitis and cirrhosis and only in one patient with fatty changes. The positivity of hepatitis markers were higher among patients with chronic hepatitis (68.2%, 4.5%, 13.64% and 13.63% for HCV Ab, HBcAb, HBsAg and both B&C respectively) and cirrhosis (42.9%, 0%, 28.6% and 28.6% for HCV Ab, HBcAb, HBsAg and both B&C respectively). Only 3(18.8%) of patients with fatty changes showed +ve HCV-ab. Hyperlipidemia & hypercholesterolemia were higher among patients with fatty changes than in chronic hepatitis and cirrhosis patients. Blood sugar was mainly elevated in fatty group.

Table(5a): Measurements of mean gray level (MGL) in 57 study subjects according to histopathological classification:

	Fatty change	Chronic hepatitis	Cirrhosis	Control
Mean±SD	30.82±1.99	28.28±2.47	29±5.38	22.53±3.75

Table(5b): The P-value of mean gray level (MGL) in different pathological and control groups:

	Fatty	Ch. Hep.	Cirr.	Control
Fatty	*	0.001	0.49	0.000
Ch. Hep.	0.001	*	0.50	0.000
Cirr.	0.49	0.50	*	0.01
Control	0.000	0.000	0.01	*

Table(5b)The mean gray level (MGL) was highest in the fatty group patients than in chronic hepatitis and control group. Also, in cirrhotic patients the MGL was significantly higher than control group subjects.

Table(6a): Measurements of 9 Th. Percentile in 57study subjects according to histopathological classification:

	Fatty change	Chronic hepatitis	Cirrhosis	Control
Mean±SD	38.18±143.06	35.68±2.91	34.814±4.35	28.4167±4.23

Table(6b): The P-value of 9 Th. Percentile in different pathological and control groups:

	Fatty	Ch. Hep.	Cirr.	Control
Fatty	*	0.02	0.09	0.000
Ch. Hep.	0.02	*	0.63	0.000
Cirr.	0.09	0.63	*	0.008
Control	0.000	0.000	0.008	*

Table(6b)The 9th Percentile of the gray level was found significantly higher in fatty, chronic hepatitis and cirrhotics, when compared to the control.

Table(7a): Measurements of contrast in 57 study subjects according to histopathological classification:

	<i>Fatty change</i>	<i>Chronic hepatitis</i>	<i>Cirrhosis</i>	<i>Control</i>
Mean±SD	49.55±8.19	51.12±9.8	55.82±14.17	39.27±9.69

Table(7a) Contrast (coarseness) was higher in cirrhosis than chronic hepatitis than fatty than control groups.

Table(7b): The P-value of contrast in different pathological and control groups:

	Fatty	Ch. Hep.	Cirr.	Control
Fatty	*	0.59	0.30	0.007
Ch. Hep.	0.59	*	0.43	0.003
Cirr.	0.30	0.43	*	0.02
Control	0.007	0.003	0.02	*

Table(7b) Contrast(coarseness) is only significantly higher in all pathological groups when compared to control group.

Table(8a): Measurements of ASM in 57 study subjects according to histopathological classification:

	<i>Fatty change</i>	<i>Chronic hepatitis</i>	<i>Cirrhosis</i>	<i>Control</i>
Mean±SD	0.0038±0.002	0.0033±0.001	0.0031±0.001	0.0044±0.001

Table(8b): The P-value of ASM in different pathological and control groups:

	Fatty	Ch. Hep.	Cirr.	Control
Fatty	*	0.16	0.13	0.33
Ch. Hep.	0.16	*	0.47	0.01
Cirr.	0.13	0.47	*	0.009
Control	0.33	0.01	0.009	*

Table (8b)The ASM was higher (more homogeneous) among fatty and chronic hepatitis group than among cirrhotic group.

Table(9a): Measurements entropy (ENT.) of in 57 study subjects according to histopathological classification:

	<i>Fatty change</i>	<i>Chronic hepatitis</i>	<i>Cirrhosis</i>	<i>Control</i>
Mean±SD	5.909±0.305	5.987±0.335	5.999±0.223	5.618±0.2565

Table(9b): The P-value of in different pathological and control groups:

	Fatty	Ch. Hep.	Cirr.	Control
Fatty	*	0.59	0.48	0.58
Ch. Hep.	0.59	*	0.90	0.003
Cirr.	0.48	0.90	*	0.000
Control	0.58	0.003	0.000	*

Table(9b)Entropy (ENT) was slightly higher among chronic hepatitis and cirrhotic groups .

Table(10a): Measurements of correlation in 57 study subjects according to histopathological classification:

	<i>Fatty change</i>	<i>Chronic hepatitis</i>	<i>Cirrhosis</i>	<i>Control</i>
Mean±SD	0.1317±0.155	0.130±0.13	0.1449±0.097	0.107±0.089

Table(10b): The P-value of correlation in different pathological and control groups:

	Fatty	Ch. Hep.	Cirr.	Control
Fatty	*	0.89	0.80	0.606
Ch. Hep.	0.98	*	0.76	0.55
Cirr.	0.80	0.76	*	0.41
Control	0.606	0.55	0.41	*

Table (11b) The correlation was found statistically indifferent in all pathological and control groups. The correlation values were found to be a little higher among cirrhotic patients

Table(11a): Measurements of attenuation coefficient (Atten) in 57 study subjects according to histopathological classification:

	<i>Fatty change</i>	<i>Cirrhosis</i>	<i>Control</i>
Mean±SD	0.570±0.055	0.482±0.03	0.476±0.04

Table(11b): The P-value of attenuation coefficient (Atten) in different pathological and control groups:

	<i>Fatty</i>	<i>Ch. Hep.</i>	<i>Cirr.</i>	<i>Control</i>
<i>Fatty</i>	*	0.90	0.000	0.000
<i>Ch. Hep.</i>	0.90	*	0.006	0.000
<i>Cirr.</i>	0.000	0.006	*	0.694
<i>Control</i>	0.000	0.000	0.694	*

Table(11b)Attenuation was found significantly higher in fatty group and chronic hepatitis group than the control group and the cirrhotic group.

Table(12a): Measurements of ID in 57 study subjects according to histopathological classification:

	<i>Fatty change</i>	<i>Chronic hepatitis</i>	<i>Cirrhosis</i>	<i>Control</i>
Mean±SD	55.87±25.98	47.76±14.06	61.87±21.47	48.07±24.84

Table(12b) The P-value of ID in different pathological and control groups:

	<i>Fatty</i>	<i>Ch. Hep.</i>	<i>Cirr.</i>	<i>Control</i>
<i>Fatty</i>	*	0.26	0.57	0.42
<i>Ch. Hep.</i>	0.26	*	0.14	0.963
<i>Cirr.</i>	0.57	0.14	*	0.22
<i>Control</i>	0.42	0.963	0.22	*

Table(12a&b)The ID value was found rather similar in all groups . No statistically significant difference was found between groups.

Table(13a): Measurements of IS in 57 study subjects according to histopathological classification:

	<i>Fatty change</i>	<i>Chronic hepatitis</i>	<i>Cirrhosis</i>	<i>Control</i>
Mean±SD	875.51±215.59	759.55±160.93	799.2±528.2	485.95±191.6

Table(13b) The P-value of IS in different pathological and control groups:

	Fatty	Ch. Hep.	Cirr.	Control
Fatty	*	0.08	0.51	0.000
Ch. Hep.	0.08	*	0.71	0.000
Cirr.	0.51	0.71	*	0.019
Control	0.000	0.000	0.019	*

Table(13b) The IS was significantly different between the pathological groups and the control group)

Table(14a): Measurements speckle separation of in 57 study subjects according to histopathological classification:

	<i>Fatty change</i>	<i>Chronic hepatitis</i>	<i>Cirrhosis</i>	<i>Control</i>
Mean±SD	2.156±1.05	2.316±0.57	2.714±0.923	1.832±0.683

Table(14b): The P-value of in different pathological and control groups:

	Fatty	Ch. Hep.	Cirr.	Control
Fatty	*	0.59	0.22	0.34
Ch. Hep.	0.59	*	0.17	0.05
Cirr.	0.22	0.17	*	0.05
Control	0.34	0.05	0.05	*

Table(14b)The speckle separation distance was found to be higher in cirrhotics and chronic hepatitis group than in fatty and control groups.

Table(15a): Measurements of speckle separation of 57 study subjects according to histopathological classification

	Fatty changes	Chronic Hepati	Cirrhosis	Control
Mean±SD	2.156±1.05	2.316±0.57	2.714±0.923	1.832±0.683

Table(15b): The P-value of speckle separation in different pthological and control group.

	Fatty	Ch.Hep.	Cirr.	Control
Fatty	*	0.59	0.22	0.34
Ch. Hep.	0.59	*	0.17	0.05
Cirr.	0.22	0.17	*	0.22

Control 0.34 0.05 0.05 *

Table(15b) No statistically significant different between all groups.

Table (16): The results of testing the efficacy the neural network in diagnosis of training set.

Group	No. of recognized cases	No. of unrecognized cases
Fatty group (10)	90%	10%
Chronic hepatitis group (12)	92.7%	8.3%
Cirrhosis group (4)	100%	0%
Control group (6)	100%	0%

Table(16) showed that the ability of the net work classifier for recognition was 90% in fatty changes 92.7% in chronic hepatitis and 100% in cirrhotic and control groups.

Table (17): The results of testing the efficacy the neural network in diagnosis of test set.

Group	No. of recognized cases	No. of unrecognized cases
Fatty group (6)	83.4%	16.6%
Chronic hepatitis group (10)	90%	10%
Cirrhosis group (3)	100%	0%
Control group (4)	100%	0%

Table (17) Showed that the ability of the net work classifier for recognition new cases, was 83.4% in fatty group, 90% in chronic hepatitis, 100% in cirrhotic and control groups.

Table (18): Assessment of sensitivity, specificity and accuracy of the neural network in the diagnosis of bright liver cases.

	Sensitivity	Specificity	Accuracy
Training set	92.30%	100%	93.75%
test set	89.47%	100%	91.3%
Overall	91.11%	100%	92.72%

DISCUSSION :

It was reported that various causes of bright liver include cirrhosis, chronic hepatitis, severe long standing cardiac failure, diffuse lymphoma, diffuse hepatocellular carcinoma, glycogen storage disease and hemochromatosis (Skolnick M., 1986). Among 41 Egyptians patients with ultrasonically detected bright liver, cirrhosis was found in (12.2%), chronic hepatitis in (51.22%), fatty liver in (34.15%) and granulomatous hepatitis in (2.43%) (Ahmed L. et al., 1993). This study included 45 patients with biopsy-proven liver disease together with 12 healthy subjects as a

control. Based on the results of liver biopsy and ultrasonographic findings, they were classified into 4 groups; fatty change group (28%), chronic hepatitis group (38.6%), cirrhotics (12.3) and controls (21%).

In this study, the mean gray level (MGL) was highest in the fatty group patients (the brightest images). It was significantly higher in the fatty group patients than in chronic hepatitis and control group. Also, in cirrhotic patients the mean gray levels were significantly higher than control group subjects. The 9th percentile of the gray level was found significantly higher in fatty, chronic hepatitis and cirrhotics, when compared to the control group. Similar results were observed by **Haberkorn et al (1990)**, they reported increase of the first order gray level statistics which correlated well with the structure as well as brightness of the ultrasound image in biopsy proven cirrhotic and fatty patients.

Layer et al. (1991) showed that the mean gray level correlates better with total lipid content than with the amount of connective tissue. Furthermore, they demonstrated, in vitro study, that connective tissue leads only to a weak increase in the mean gray level, whereas the addition of connective tissue to a given tissue lipid can lead to a reduction in image brightness.

The parameters taken from the histogram can not be used to quantify the number, size and orientation of localized texture structures in the image due to lack of spatial information. That is why we need parameters from the co-occurrence matrix which is a two-dimensional histogram characterizing the occurrence gray level combinations in pairs of spatially related pixels (**Layer et al., 1990**).

In this study, contrast, entropy, correlation and angular second moment were extracted from the co-occurrence matrix. These parameters measure not only the occurrence frequencies of gray levels but also used the spatial interdependencies between the image elements (pixels).

Contrast defines the coarseness of texture. Frequently occurring large gray level differences increase the contrast value, whereas soft texture results in small contrast value (**Raeth et al., 1985**). It was higher in cirrhosis and chronic hepatitis group than fatty and control groups. This may be due to large gray level difference between fibrous tissue and surrounding parenchyma in cirrhotic patients.

Angular second moment(ASM) and entropy characterizes the distribution of co-occurrence matrix in a gray level-independent way. Angular second moment increases when the co-occurrence matrix values are clustering around a major gray level transition. This corresponds to a situation where only a small number of different gray level transitions exist (i.e., homogeneity). Among our patients the ASM was higher (more homogeneous) among fatty and chronic hepatitis group than among cirrhotic group (see table 9). Entropy measures the homogeneity or uniformity of the image elements (pixels) and therefore it increases with increasing coarseness of the image texture (Raeth et al., 1985). So, it was suspected to be significantly higher in cirrhotic group due to the coarse texture. However, it was slightly higher among chronic hepatitis and cirrhotic groups. This may be due the majority of patients were in the early stages and cases with coarse echopattern were excluded.

Correlation measures the linearity of the relationship of the gray levels in d-related pixels. In homogeneous texture the transitions in the difference between the gray levels between neighboring pixels are little (i.e. low correlation values), while in coarse texture, the transitions of gray levels are frequent (i.e. high correlation values) (Badawi et al., 1996). In our study the correlation was found statistically indifferent in all pathological and control groups. However, the correlation values were found to be a little higher among cirrhotic patients. These results may also be due to the early cirrhotic cases found.

Attenuation is simply the loss of energy of an ultrasound signal as it is propagated through tissue. In this study, the estimated mean attenuation value for control cases was 0.476 ± 0.04 dB/cm./MHz. The attenuation of normal liver has generally been reported to be between 0.5 and 0.6 dB/cm./MHz. Higher values for attenuation were reported in the early literature yet rather recent literature suggested that attenuation in normal liver is approximately 0.5 dB/cm./MHz (Garra, 1991).

In vivo work by Lin et al. (1988) demonstrated that both fibrosis and fatty infiltration produced increased attenuation. In this study, Attenuation was found significantly higher in fatty group and chronic hepatitis group than the control group and the cirrhotic group. These results are in agreement with Parker et al. (1988a&b) who confirmed elevated attenuation in fatty livers and suggested that fibrosis could also produce elevated attenuation values. Also, Garra (1991) suggested that elevated attenuation in cirrhotics be primarily due to concomitant fatty infiltration with fibrosis,

playing a smaller role (if any).

On the other hand, **Lin et al. (1988)** stated that cirrhotics had elevated attenuation values. In summary, attenuation estimation has made it possible to separate normal livers from certain disease states. Unfortunately, in the liver, elevated attenuation appears to be primarily related to fatty infiltration rather than the more important changes of inflammation and fibrosis. This severely limits the usefulness of attenuation estimation for the characterization of liver disease.

The granular texture of ultrasonic images has become known as ultrasonic speckle. The tissue scatters vary in size and shape and those different structures have varying degrees of spatial order. A simple biological scattering medium is blood where the scatters are small and completely disordered. Ultrasonic backscatter from this type of material is known as Rayleigh (random) scattering in which a histogram of pixel intensities of random (diffuse) scatters (I_d) follows a characteristic distribution. In addition to random scatters, most biological tissues also have another two types of non-random (specular) scatters: those of one type are ordered over very short distances such as those composing the walls of blood vessels and organ, the second type are organized over longer distances and contribute a specular backscatter intensity (I_s).

Tissue characterization features based on the relative contributions of intensities from diffuse scatters and specular scatterers may be estimated using the average autocorrelation function. From the autocorrelation function and speckle power spectrum I_d and I_s are obtained. These quantities have been tested on patient data and have been found to be useful for separating normal from diseased liver tissue (**Wagner, 1987**).

Garra, (1989) found that I_s/I_d (the ratio of specular to diffuse backscatter intensities) is a measure of the variability in the specular component to detect various types of diffuse liver diseases. However, in our study no statistically significant difference between pathological groups were observed.

The speckle separation distance is the average distance between regularly positioned specular scatters (mean scatterer distance). It can be measured from the speckle power spectrum.

In this study, the speckle separation distance was found to be higher in cirrhotics and chronic hepatitis group than in fatty and control groups. This was similar to results obtained by **Fellingham and Sommer (1984)**. They found that the mean scatter spacing was significantly increased in patients with liver cirrhosis when compared to healthy subjects. This was explained by the coarse texture observed in these cases. These results are also similar to those obtained by **Suzuki et al. (1991)** who found that The spaces between scatterers for liver cirrhosis was significantly larger than that for chronic hepatitis and nonspecific change.

The sensitivity (91.11%), specificity (100%) and accuracy (92.72%) obtained in this study for diagnosis of diffuse liver diseases presented by bright liver in their ultrasonic examination is greater than the results obtained by conventional ultrasonography (70%), and comparable to results obtained by computer assisted studies for authors as: **Rath et al. (1984)** reported (85%,95%,90%), **King et al. (1985)** reported (88%,100%,95%), **Schuster et al., (1988)** reported (94-97%,87-100%,90-98%).

We concluded that computer-assisted sonographic tissue characterization using the neural network classifier is a sensitive and specific technique for separating diffuse liver disease namely; fatty, cirrhotic, chronic active hepatitis cases with ultrasonically detected bright liver from control cases. We may recommend to increase number of cases and number of pathological classes for example mixed liver pathology so as to increase sensitivity, specificity and overall accuracy which may replace histopathology in the future. We also recommend the application of this computerized system for automatic diagnosis of focal liver diseases.

REFERENCES:

1. **Ahmed L., Salama H., Medhat E. and Khalil A.**, "Assessment of ultrasonically detected bright non-chronic liver among Egyptian patient", *J. Egypt. Med. Assoc.* 78 (1-6) 175:184, 1995.
 2. **Badawi A. M., Salim M. Emara and Abou-Bakr M. Youssef**, "Ultrasound Tissue Characterization of Diffuse Liver Diseases Using Fuzzy Rules", *International Fuzzy Systems and Intelligent Control Conf. (IFSIC)*, 1994.
-

3. **Badawi A. M.**, "Quantitative techniques and algorithms for ultrasound tissue characterization of diffuse liver disease", Ph.D. Thesis, Cairo Univ., Dept. of Biomedical. Eng. Cairo 1996.
 4. **Badawi A. M., Derbala A. S., and Youssef A. M.**, "Fuzzy logic algorithm for quantitative tissue characterization of diffuse liver diseases from ultrasound images." *Int. J. Med. Inf.*, Aug., 55 (2): 135-47, 1999.
 5. **Behan M. and Kazam E.** "The echogenic characteristics of fatty tissues and tumors", *Radiology*, 129:143-149, 1978.
 6. **Brailton, A., Capron, J.P., Herve, M.A., Degott, C. and Quenum, C.** "Liver in obesity." *Gut*, 62, 133-139, 1985.
 7. **Dewbury, K.C. and Clark, M.B.** "The accuracy of ultrasound in the detection of cirrhosis of the liver" *British Journal of Radiology*, 52: 945-948, 1979.
 8. **El-Rooby, A.S.** "Management of hepatic schistosomiasis." *Seminars in Liver Diseases*, 5: 263-275, 1985.
 9. **Fellingham, L.L. and Sommer, F.G.** "Ultrasonic characterization of tissue structure in the human liver and spleen" *IEEE Transactions in Sonics and Ultrasonics* (Supplement 31): 418 - 428, 1984.
 10. **Franzese A., Vajro P., Argenziano A., et al.** "Liver involvement in obese children, Ultrasonography and liver enzyme levels at diagnosis and during follow-up in an Italian population". *Dig. Dis. Sci.*, Jul, 42(7):1428-32, 1997.
 11. **Garra, B.S., Insana, M., Shawker, T.H. et al.** "Quantitative ultrasonic detection and classification of diffuse liver diseases: Comparison with human observer performance" *Invest. Radiol.*, 24:196-203, 1989.
 12. **Garra, B.S.**, In vivo liver and splenic tissue characterization by scattering"" (draft of a book to be published). . 1991, Special communication with Prof. Esmat, G.
 13. **Gosink, B.B., Lemon, Scheiblexw. and Leopold, G.R.** "Accuracy of ultrasonography in diagnosis of hepatocellular diseases" *AJR*, 133: 19, 1979.
 14. **Haberkorn, U., Zuna, I., Loreuz, A. et al.** "Echographic tissue characterization in diffuse parenchymal liver disease: correlation of image structure with histology." *Ultrason. Imaging*, Jul, 12:3, 155-70, 1990.
 15. **Joseph, A.E.A., Dewbury, K.C. and Mc Guire, P.G.** "Ultrasound in the detection of chronic liver disease (the "bright liver")", *British Journal of Radiology*, 52: 184-188, 1979.
 16. **Kadah Y. M. , Badawi A. M. , et al.** "Quantitative techniques and algorithms for ultrasound tissue characterization of diffused liver diseases", *IEEE Med Imag.*, August 1996.
-

17. King, D.L., Lizzi, F.L., Feleppa, E.J. et al. "Focal and diffuse liver disease studied by quantitative microstructural sonography. " *Radiology*; 155: 457-462, 1985.
 18. Layer, G., Zuna, I., Lorenz, A. et al. "Computerized ultrasound B-scan texture analysis of experimental fatty liver disease: influence of total lipid content and fat deposit distribution" *Ultrason. Imaging*, Jul; 12(3):171-88, 1990.
 19. Layer, G., Zuna, I., Lorenz, A. et al. "Computerized ultrasound B-scan texture analysis of experimental diffuse parenchymal liver disease: correlation with histopathology and tissue composition.", *J Clin Ultrasound* May;19(4):193-201, 1991.
 20. Lin, T., Ophir, J. and Potter, G., "Correlation of ultrasonic attenuation with pathologic fat and fibrosis in liver disease" *Ultrasound in Medicine and Biology*, 14: 729-734, 1988.
 21. Parker, K.J., Asztely, M.S., Lerner, R.M., Schenk, E.A. and Waag, R.C. "In-vivo measurements of ultrasound attenuation in normal and diseased liver" *Ultrasound in Medicine and Biology*, 14: 127-136, 1988a.
 22. Parker, K.J., Lerner, R.M. and Waag, R.C. "Comparison of techniques for in-vivo attenuation measurements", *IEEE Transactions on Biomedical Engineering*, 35: 1064 -1067, 1988 b.
 23. Raeth U., Schlaps D., Limberg B. et al. "Diagnostic accuracy of computerized B-scan texture analysis and conventional ultrasonography in diffuse parenchymal and malignant liver disease", *J. Clin. Ultrasound*, 13:87-99, 1985.
 24. Rath, U., Chlapy, D., Limberg, B., et al. "Diagnostic accuracy of computerized B-scan texture analysis and conventional ultrasonography in diffuse parenchymal and malignant liver disease." *Journal of Clinical Ultrasound*, 13: 87-99, 1985.
 25. Rath, U., Zuna, L., Limberg, B., et al. "Der Beitrag der Grauwertistogramm-Analyse zur sonographischen Diagnostik des diffusen Leberparenchymschadens." *Abstr. Ultraschall in der Medizin*, 5: 94 - 97, 1984.
 26. Schuster, E., Knoflach, P., Huber, K. and Grabner, G., "An interactive processing system for ultrasonic compound imaging, real-time processing and texture analysis." *Ultrasonic Imaging*, 8: 131-150, 1986.
 27. Schuster, E., Knoflach, P. and Grabner, G. "Local texture analysis: an approach to differentiating liver tissue objectively." *J Clin Ultrasound* Sep; 16(7):453-61, 1988.
 28. Sherlock, S. and Dooley, J. "Diseases of the liver and biliary system." Ninth edition. Blackwell scientific publications.1997.
-

29. *Skolnick, M. L.* "Guide to ultrasound examination of the abdomen" Ch. 7: 87- 88. Springer Verlag, 1986.
 30. *Suzuki, K., Hayashi, N., Sasaki, Y. et al.* "Ultrasonic tissue characterization of chronic liver disease using cepstral analysis", *Gastroenterology*, Nov, 101:5, 1325-31,1991.
 31. *Wagner, R.F., Insana, M.F. and Brown, D.* "Statistical properties of radio-frequency and envelop-detected signals with applications to medical ultrasound" *J Opt. Soc. Am. A.* 4:910-922, 1987, (abstr.).
 32. *Youssef A. M. and Badawi A. M.*, "Tissue characterization of Diffuse Liver Diseases Using Neural Nets", Annual meeting of Egyptian Society of hepatology & gastroentreology, 1993.
 33. *Youssef A. M. and Badawi A. M.*, "Improved B-Scan Images Using Ultrasound Average Attenuation with Correlation to Diffuse Liver Diseases", Annual meeting of Egyptian Society of hepatology & gastroentreology, 1993.
 34. *Zwiebel, W.J.* "Sonographic diagnosis of diffuse liver disease." *Seminars in Ultrasound, CT and MRI*, 16: 8-15, 1995.
-